LADDER FILTERS

Ladder filters are an important class of filter structures for implementing highly selective magnitude frequency responses. If the ladder filter structure is used to implement or simulate resistively terminated reactive *LC* filters, desirable properties, such as the inherent stability and low sensitivity with respect to parameter changes, can be retained.

The first *LC* ladder filters were implemented using inductors (*L*'s) and capacitors (*C*'s), operating in the continuous-time domain and embedded between resistive terminations. They are referred to as analog or classical *LC* ladder filters. These classical *LC* ladder filters perform remarkably well in practice and are capable of realizing highly selective magnitude frequency responses. However, they are not suitable for microelectronic integration because inductors are usually bulky. To overcome this limitation, inductorless microelectronic filters, such as *RC*-active filters, switched capacitor (SC) filters, and digital filters, have been developed. In the early years of their development, these modern microelectronic filters were unfortunately found to be inferior to *LC* ladder filters for a number of reasons. In particular, they did not possess the desired inherent stability and low-parameter sensitivity properties and, as a result, had poor performance in terms of stability and parameter sensitivity, especially for realizing highly selective magnitude frequency responses.

Fortunately, it has been found that the superior classical *LC* ladder filter structure and its corresponding filter design methodology can be simulated by modern microelectronic filters. For example, the desired properties of passivity and losslessness, as possessed by *LC* ladder filters, can be extended to modern microelectronic filters in order to ensure stability and to significantly improve the sensitivity performance of the filter.

In this article, we are concerned with the design, synthesis, and implementation of ladder filters that conform to or simulate the ladder structure. We shall explain the general features of the ladder structure and its inherent advantages as well as its most successful and widely used technological implementations such as reactive *LC*, *RC*-active, SC, and digital filters. We begin with an overview of this subject and by placing the subject in its historical context.

OVERVIEW OF LADDER FILTERS

The Historical Development of Classical *LC* Ladder Filters (1,2)

Filter theory was developed at a remarkable pace in the early years of the twentieth century. By 1915, Campbell and Wagner had developed the first *LC* filter, which not coincidentally was a ladder implementation. The first systematic *LC* ladder filter design technique was facilitated by image parameter theory as introduced by Zobel in 1923. This theory was further refined by Bode and Piloty in the 1930s. The resulting classical ladder filter design technique was employed extensively until the 1960s when the digital computer made alternative filter design techniques practical.

The image parameter method helped to develop an intuitive approach to the filter design problem without requiring a computer. However, it was an approximate method which did not make effective use of the poles and zeros that are provided by the filter transfer function, resulting in suboptimal designs in terms of the order of the filter. Therefore, much research was devoted to finding an optimal solution for the *LC* ladder filter design problem, including both the approximation of the filter transfer function and the synthesis of the *LC* ladder filter network.

In 1924 and 1926, a major advance occurred when Foster and Cauer invented canonical one-port *LC* networks, essentially solving the general one-port *LC* synthesis problem. Later, in 1931, the general passive one-port synthesis problem was solved by Brune. His solution led to the fundamentally important concept of the positive real function, which became the most important mathematical vehicle for the design of *LC* filters and which continues to be the basis of many alternative techniques for designing high-performance *RC*-active, SC, and digital filters. In 1930, Butterworth and Cauer introduced the maximally flat and Chebyshev approximations of the filter transfer function, respectively, thereby solving the approximation problem for an important class of filters. In 1937, Norton proposed a new filter design approach which started from a prescribed insertion loss function. The general reactance two-port synthesis problem, which was involved in this new filter design method, was solved independently by a number of researchers between 1938 and 1941. In particular, Darlington and Cauer's work led to optimal *LC* ladder filters that are now widely known as *elliptic filters.* The insertion loss theory of filter design was further developed by Belevitch in 1948 using scattering matrix theory, which evolved to become the most important *LC* filter design method. However, because of the extensive numerical computations that this technique involved, it only found wide applications when powerful digital computers became available in the 1960s.

The Properties and Classical Implementations of *LC* Ladder Filters

The classical *LC* filter is a two-port reactance (thus lossless) network N that consists of ideal inductors and capacitors and that is inserted between a voltage source E and two terminating resistors such as shown in Fig. 1(a), where the uppercase voltages indicate steady-state voltages. If this two-port N is a ladder structure, then it consists of alternating series and shunt branches and is referred to as a double-resistively terminated ladder filter. For *LC* ladder filters, the series and shunt branches are made up of simple inductors and capacitors or simple parallel and series resonant circuits. An example of a fifth-order *LC* ladder filter is shown in Fig. 1(a). This filter structure is widely used to implement the elliptic filter transfer function, whose typical attenuation response is shown in Fig. 1(b).

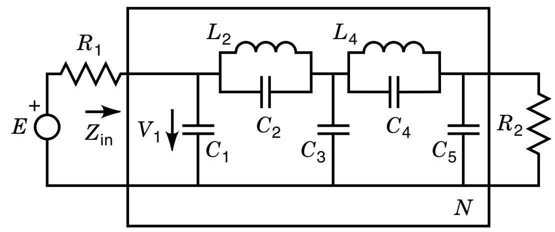

(a)

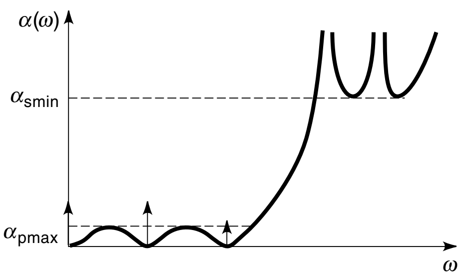

(b)

Figure 1. (a) A fifth-order ladder two-port N inserted between resistive terminations. (b) Attenuation response of a fifth-order elliptic filter. The arrows indicate possible shifts of attenuation caused by changes of filter parameter values.

The LC ladder filter structure is widely considered to be a preferred filter structure because of its many inherently useful properties. Apart from the inherent advantages of the ladder topology, the properties of passivity and losslessness are of particular significance. First, the individual inductor and capacitor components of the embedded LC ladder network are passive and lossless, implying (according to Kirchhoff's voltage and current laws) that the complete LC ladder filter is passive and lossless. It is very important to note that the LC ladder network actually satisfies a more stringent passivity/losslessness definition, namely the internal passivity/losslessness. A Kirchhoff's network is internally passive/lossless if and only if all the individual internal components are passive/lossless. By proper design, the property of internal passivity/losslessness guarantees stability and freedom from parasitic oscillations for the filter realizations that are subject to parasitic effects. Filters, in particular, RC-active, SC, and digital filters, which do not simulate the internal passivity/losslessness, are subject to (usually nonlinear) instability problems that are caused by such parasitic effects as nonideal phase shift, saturation, and lock-up of op-amps or quantization effects in digital filters. It is important to note that the simulated internal passivity/losslessness must be retained when internal filter parameters are parasitically perturbed from their nominal values.

In the early years, the inductors and capacitors within LC ladder filters were implemented using coils and condensers, respectively, and could not be manufactured to the level of precision that is achievalble today. However, the attenuation responses of those early LC ladder filters did not show high sensitivity with respect to the LC component values and the filters performed surprisingly well in practice. The theoretical explanation for this remarkable property, which may be explained in terms of the first-order sensitivity property, has been given by Fettweis (3) and Orchard (4) and is summarized in the following.

The filter transfer function of the reactance two-port N such as shown in Fig. 1(a) is characterized by

$$S_{21} = \frac{2\sqrt{R_1/R_2}V_2}{E} \tag{1}$$

In the terminology of scattering matrix theory, S_{21} is called the input–output transmittance or the transmission coefficient. The filter attenuation response α, corresponding to S_{21}, is given by

$$\alpha = 10\log(1/|S_{21}|^2) = 10\log(P_{max}/P_2) \tag{2}$$

where $P_{max} = |E|^2/4R_1$ is the maximum power available from the voltage source and $P_2 = |V_2|^2/R_2$ is the power delivered to the load resistor. Because a reactance two-port is lossless and therefore passive, we have $P_2 \le P_{max}$ and therefore $\alpha \ge 0$. Let x be any internal component value such as an inductance or capacitance inside the reactance two-port. If for a particular value of x, say x_0, we have $\alpha = 0$ at a certain frequency ω_0, the attenuation $\alpha(\omega_0, x)$, which is a function of x with a fixed parameter ω_0, has a minimum at $x = x_0$. This leads to $\partial\alpha(\omega_0, x)/\partial x = 0$ for $x = x_0$, and in general, $\partial\alpha/\partial x = 0$ for $\alpha = 0$ and $\partial\alpha/\partial x \approx 0$ for $\alpha \approx 0$. This shows that, for a well-designed lossless LC filter network (i.e., having an attenuation response with the maximum number of attenuation zeros at real frequencies in the passband etc.), the first-order sensitivity of the attenuation response with respect to any LC component value is small everywhere in the passband; furthermore, the closer the attenuation response is to its limiting value of zero, the smaller the sensitivity of the attenuation to perturbations of x. Furthermore, this low passband-sensitivity property can be shown to lead to excellent noise immunity and superior dynamic range.

In addition to the above-mentioned property of low sensitivity in the passband, LC ladder filters also exhibit superior low-sensitivity performance in the stopband, compared with many other lossless filter structures, such as lattice structures. Although the above lossless argument establishes the low passband-sensitivity property, it does not apply to the stopband; in fact, the low stopband sensitivity is a result of the unique ladder topology, as explained in the following.

Let us consider the filter network in Fig. 1(a). In the passband, the transmitted power P_2 closely approximates the maximum available power P_{max}, and P_2 indeed equals P_{max} at the attenuation zeros. This means that the input impedance Z_{in} equals R_1 at those zeros. In the stopband, the attenuation poles are attributed, in a one-to-one correspondence, to the reactance poles in the series branches and susceptance poles in the shunt branches. These poles disconnect the series branches and short-circuit the shunt branches, respectively. Therefore, the location of each attenuation pole is independently determined by a particular series reactance or shunt susceptance. Furthermore, because the series reactance and the shunt susceptance are usually either a single inductor/capacitor or a simple resonant circuit, the reactance/susceptance and thus the locations of attenuation poles are easily tuned. Furthermore, the deviation of poles with respect to their ideal locations, due to perturbations of LC component values, is small if the change of the component values is small. In general, the series/shunt reactances/susceptances are implemented using the Foster canonical forms, which guarantee that the reactance/susceptance poles are independent of each other and are attributed to either a single inductor/capacitor or to a single second-order resonant circuits. Therefore, the sensitivity of the locations of attenuation poles with respect to changes of component values is low for *LC* ladder filters. This leads to the low stopband sensitivity for *LC* ladder filters, because the attenuation response in the stopband is mainly determined by the number and the locations of attenuation poles.

The low stopband sensitivity of *LC* ladder filters is superior to that of other types of *LC* filters, such as *LC* lattice filters. In *LC* lattice filters, the attenuation poles are achieved by signal cancellation of two or more transmission paths, causing the above-mentioned superior stopband sensitivity property to be lost. As a result of this relatively poor stopband sensitivity performance, classical *LC* lattice filters are used in special cases where the problem can be contained. For example, modern digital techniques have revitalized *LC* lattice filter structures, because the high stopband-sensitivity may be alleviated by means of appropriate discrete numerical optimization techniques.

Classical *LC* ladder filters are implemented by using discrete inductors and capacitors, usually mounted on printed circuit boards. Continued advances in materials research have led to small and inexpensive *LC* components of very high quality. Filter designers can refer to practical guides, such as Ref. 5, in order to select the *LC* values and parts and to find information on testing and manufacturing.

Modern Implementations of Ladder Filters

The invention of transistors in the 1950s has played an important role in the integrated circuit revolution and, in particular, has fueled the pervasive growth of the modern computer and telecommunications industries. In spite of the high demand for filter systems in microelectronic form and the above-mentioned attractive properties of classical *LC* ladder filters, the integration of the inductor has generally proven to be impractical, thereby preventing the application of classical *LC* filters in microelectronic forms. This limitation of classical *LC* filters led to much research on the topic of inductorless filters.

In the 1950s, Yanagisawa and Linvill pioneered the field of *RC*-active filters and showed that passive *RC* elements and active controlled voltage or current sources could be combined to realize general filter transfer functions. Sallen and Key proposed a single-amplifier configuration for realizing second-order transfer functions, which were very useful for implementing low-order low-sensitivity filter transfer functions. Nevertheless, these early *RC*-active filters proved to be overly sensitive with respect to changes of component values for applications involving high order and highly selective transfer functions. Moreover, they also required impractically large spreads of component values and had a tendency to be unstable due to parasitics.

In the 1960s, the availability of high-performance microelectronic operational amplifiers (op-amps) allowed single op-amp *RC*-active filters to be used in many applications. In the 1970s and 1980s, the cost of op-amps declined dramatically whereas the precision *RC* elements, as required by this type of *RC*-active filters, remained expensive, thereby lending significant advantage to multiple-amplifier filter implementations that allowed low-cost *RC* elements to be used. The *RC*-active filters that are based on simulating classical *LC* ladder filters possess this very property and thus have been rapidly developed.

There are two basic *LC* ladder simulation techniques. One technique is based on simulating the *LC* ladder signal flow graphs (SFG) and is referred to as the operational simulation technique. The other is based on simulating the inductors in the *LC* ladders and is referred to as the component simulation technique. The inductor simulation technique is best explained by using the concept of the two-port gyrator, which was originally proposed by Tellegen in 1948 and led to the invention of active generalized impedance converters (GIC) by Riordan (6) and Antoniou. An alternative inductor simulation technique is to use the so-called frequency-dependent negative resistance (FDNR) elements, which were invented by Bruton. These methods are discussed later in this article, along with other modern ladder filter implementations. In Ref. 7, a historical review of the development of *RC*-active filters and a large number of references are listed.

In the 1970s, the pervasive MOS technology offered new opportunities for making microelectronic active ladder filters because low-power amplifiers and highly accurate capacitor ratios could be made at very low cost and at very high density by using the same fabrication process. These technical advances led to the development of SC filters, where capacitors and switches were initially used to replace the resistors in *RC*-active filter configurations.

In general, the voltages in SC filters are ideally constant except at the instants of time when switches are caused to open or close. Thus, the voltages waveforms are sampled-data staircase waveforms that are related to each other by the same family of linear difference equations that describe the relationships between the variables of digital filters. A historical review of the development of SC filters is given in Refs. 8–10.

While SC filters are analog sampled data systems, digital filters are quantized sampled data systems. The widely spread industrial applications of digital filters have been enabled by the invention of CMOS VLSI technology in the 1980s. Digital filters have the advantage over analog filters that they do not suffer from manufacturing and temperature variations and aging effects. This advantage of digital filters provides an opportunity to exploit the higher-order low-passband-sensitivity property of classical *LC* filters (11) when designing digital filters to simulate classical lossless *LC* filters, such as wave digital filters (WDF) which were invented by Fettweis and lossless discrete integrator/differentiator (LDI/LDD) digital filters which were invented by Bruton. A technical review of digital filters and a large number of references can be found in Ref. 12.

The benefits of using high-order low passband sensitivity are considerably greater than might be expected from the first-order sensitivity property discussed in the previous section. To show this, let us consider the attenuation response of the lossless filter $\alpha(\omega, x_0)$ again, where x_0 indicates any original digital filter coefficient value. If x_0 changes to $x_0 + \Delta x$ in such a way that the losslessness is maintained, $\alpha(\omega, x_0 + \Delta x) \geq 0$ still holds for the resulting attenuation response. In this case, the size of Δx does not have to be small and the attenuation minima can only shift in the same upward direction [see Fig. 1(b)]. The resulting attenuation distortion $\Delta\alpha$ is predominantly determined by the differences of these shifts and is therefore smaller, possibly substantially smaller, than the individual changes of the minima. Because, once the filter coefficients are determined, the attenuation responses of digital filters do not change due to manufacturing process, temperature, and aging, this higher-order low passband sensitivity can be used for the discrete optimization of filter coefficients to obtain extremely simple-valued coefficients, thus minimizing the hardware complexity of digital filter implementations.

High-order direct-form recursive digital filters suffer from poor sensitivity performance, limit cycle, and parasitic oscillatory problems, due to underflow/overflow and high noise distortion. However, due to the internal passivity property of classical *LC* filters, digital filters that are properly derived from *LC* ladder filters, such as WDFs, can be made free from parasitic oscillations even under extremely difficult looped conditions. It is noted that in order to obtain superior performance, passivity or losslessness must be maintained under quantized conditions and considerable design effort may be required to ensure that this is achieved.

The above-mentioned benefits of digital filters were often offset by the requirement for relatively expensive analog-to-digital and digital-to-analog converters (ADC and DAC) and by the relatively high cost of digital filters. However, during the 1990s, the advent of deep-submicron CMOS VLSI technology has virtually reversed the cost equation in favor of digital filters. Moreover, the transition of the computer and telecommunications industries to entirely digital systems has eliminated the need for local ADCs and DACs and, in many cases, has dictated the use of digital filters. The use of analog continuous-time filters, such as *LC*, *RC*-active, and SC filters, may soon be restricted to ultrahigh-frequency applications where sampling and digitization are not economical or feasible. For example, front-end analog radio-frequency (RF) filters in wireless systems are typically implemented as analog circuits because small low-valued RF inductors may be made at low cost. Furthermore, RF resonator-type ladder filters such as surface acoustic wave (SAW) ladder filters find wide applications in wireless systems. In this type of filters, the ladder branches consist of (SAW) resonators, and the corresponding filter design procedure has many similarities to the image parameter method.

ON THE DESIGN OF PASSIVE *LC* LADDER FILTERS

The design of modern microelectronic ladder filters is based on the same underlying approximation theory and ladder synthesis methods that are used to design classical *LC* ladder filters. The values of ladder elements for prototype low-pass filters are tabulated in design handbooks (13,14). High-pass, band-pass, and band-stop filters are often derived from prototype low-pass filters using frequency transformation techniques. Alternatively, the filter approximation and synthesis can also be performed by filter design software packages. In this section we will briefly discuss the underlining principles of filter approximation theory and the ladder synthesis techniques that lead to optimal *LC* ladder filter structures. The interested readers may consult related articles in this encyclopedia and Refs. 15–19 for a more comprehensive treatment of this topic.

The General Design Procedure

There are two steps in designing a filter. The first step is to find a transfer function having a frequency response that satisfies the specified attenuation and/or phase response requirements. The second step is to synthesize a filter network that realizes this transfer function. In the case of *LC* ladder filters, the filter transfer function is realized using an *LC* ladder network. In the following, we review the method of determining the filter transfer function and the ladder synthesis technique for *LC* filters.

The double-resistively terminated filter network N in Fig. 1(a) possesses transmittance S_{21} as defined in Eq. (1) and reflectance (or the reflection coefficient) S_{11}, which is defined as

$$S_{11} = (2V_1 - E)/E$$

For *LC* ladder filters, the embedded network N is lossless. Therefore, no power is dissipated in the network N. Thus, the two transfer functions S_{11} and S_{21} are complementary, implying that

$$|S_{11}(j\omega)|^2 + |S_{21}(j\omega)|^2 = 1 \tag{3}$$

By introducing a new variable $C = S_{11}/S_{21}$ and by taking Eq. (3) into account, the attenuation response given by Eq. (2) can be rewritten as

$$\alpha(\omega) = 10\log(1/|S_{21}(\omega)|^2) = 10\log(1 + |C(j\omega)|^2) \tag{4}$$

The function $C(j\omega)$ is the so-called characteristic function having zeros and poles that correspond with those of the attenuation response $\alpha(\omega)$. This one-to-one correspondence of zeros and poles between the characteristic function and the attenuation response makes the characteristic function an important and sufficient choice for approximating the filter transfer function. It can be shown (18) that for lossless filters the transmittance S_{21} and the reflectance S_{11} are rational functions in the complex frequency s ($s = \sigma + j\omega$) and that S_{21} and S_{11} have the common denominator polynomial g, where g is a Hurwitz polynomial. Let

$$S_{21} = f/g \tag{5a}$$

$$S_{11} = h/g \tag{5b}$$

The characteristic function C becomes

$$C = h/f \tag{6}$$

which is also a rational function. It can be shown from Eqs. (3) and (5) that the following fundamentally important relation holds between f, h, and g for the entire s domain:

$$f(s)f(-s) + h(s)h(-s) = g(s)g(-s) \tag{7}$$

Furthermore, for *LC* filters, $f(s)$ is either an even or an odd function of s because of the reciprocity property of embedded *LC* two-ports. Now, the transfer function approximation problem can be formulated so as to find the rational functions $h(j\omega)$, $f(j\omega)$ and thereby $|C(j\omega)|^2 = h(j\omega)h(-j\omega)/f(j\omega)f(-j\omega)$

such that the attenuation response $\alpha(\omega)$, as defined by Eq. (4), satisfies the specified attenuation requirements. The fact that $g(s)$ is a Hurwitz polynomial, having its zeros in the left half of the s plane, allows itself to be obtained by solving the equation $f(s)f(-s) + h(s)h(-s) = 0$. Subsequently, the functions S_{21} and S_{11} are fully determined. Note that we have omitted discussion of phase responses because the phase response requirements for a ladder filter are usually satisfied by cascading an equalizing all-pass filter. Nevertheless, special ladder filters may be designed to satisfy the phase response requirements, such as the Thomson filter that is discussed in the following.

The transfer function approximation problem, which is the determination of the characteristic function C, was solved for low-pass filters by Butterworth, Cauer, Thomson, and others in the early years of filter design. In the next section, we discuss design examples for low-pass prototype filters where it is understood that simple frequency transformations are used to obtain high-pass, band-pass, and band-stop filters from low-pass prototype filters.

The synthesis of the double-resistively terminated two-port N in Fig. 1(a) is facilitated by the LC one-port synthesis techniques as developed by Foster and Cauer. A reactance function, which is obtained as the input immitance of an LC one-port, can always be realized in the Foster and Cauer canonical forms. The first and second Foster canonical forms are based on the partial fraction expansion of the reactance function, and the first and second Cauer canonical forms are based on the continued fraction expansion. It can be shown that a reactance function can be written in the following partial fraction form as the impedance function

$$Z(s) = B_\infty s + B_0/s + \sum_{i=1}^{n} 2B_i s/(s^2 + \omega_i^2)$$

or admittance function

$$Y(s) = D_\infty s + D_0/s + \sum_{i=1}^{n} 2D_i s/(s^2 + \omega_i^2)$$

leading directly to the first and second Foster canonical forms as shown in Fig. 2(a). Similarly, the reactance function can

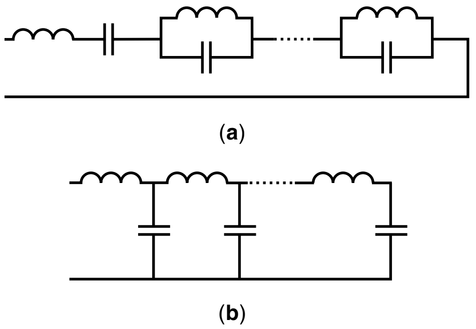

Figure 2. (a) The first Foster canonical form. (b) The first Cauer canonical form. The second canonical form is the dual network to the first canonical form. The Foster canonical forms implement each reactance/susceptance pole by a separate second-order resonant circuit. The Cauer canonical forms have a ladder structure.

also be written as continued fractions

$$Z(s) = L_1 s + \cfrac{1}{C_2 s + \cfrac{1}{L_3 s + \cfrac{1}{C_4 s + \cfrac{1}{\ddots}}}} \tag{8a}$$

or

$$Z(s) = \frac{1}{C_1' s} + \cfrac{1}{\cfrac{1}{L_2' s} + \cfrac{1}{\cfrac{1}{C_3' s} + \cfrac{1}{\cfrac{1}{L_4' s} + \cfrac{1}{\ddots}}}} \tag{8b}$$

leading directly to the first and second Cauer canonical forms shown in Fig. 2(b).

The Cauer canonical forms are reactance one-ports having a ladder structure. The continued fraction expansion technique is especially useful for synthesizing resistively terminated two-port ladder network. It can be shown that the reflectance S_{11} can be written as

$$S_{11} = (Z_{in} - R_1)/(Z_{in} + R_1) \tag{9a}$$

so that Z_{in} can be written as

$$Z_{in} = R_1(1 + S_{11})/(1 - S_{11}) \tag{9b}$$

However, Z_{in} is an impedance function and thus a rational positive real function which, according to Darlington's theory, can always be synthesized as a lossless two-port network terminated by a resistive load.

In general, the resulting two-port network involves the so-called Brune section, which is a second-order two-port network containing coupled inductors or ideal transformers, and thus strictly does not have the LC ladder structure according to our definition. However, in most cases, an LC ladder structure can be found for the input impedance Z_{in} that results from the reflectance S_{11} of a practical low-pass filter. This is especially true if the resulting two-port is allowed to be a noncanonical network. In fact, the continued fraction expansion technique, illustrated by Eq. (8), can be applied to Z_{in} in order to realize an LC ladder two-port that is terminated by a resistor.

The continued fraction expansion technique is also referred to as the pole removal technique because it removes the attenuation poles of the filter one by one during the course of the fractional expansion. For low-pass filters, having multiple attenuation poles at infinity, each step in fractional expansion removes a full attenuation pole at infinity, resulting in a canonical implementation. For low-pass filters that have attenuation poles located at finite frequencies, the removal of a finite frequency pole has to be accompanied by a partial removal of an infinity pole, in order to avoid the Brune section and to obtain a ladder structure. Because of this partial pole removal, the resulting LC ladder two-port is a noncanonical network. We will consider examples for LC ladder synthesis in the following section.

Low-Pass Prototype Filters

The most widely used low-pass prototype filters are the Butterworth, (inverse) Chebyshev, elliptic, and Thomson filters. Each of these filters has particular characteristics that may be preferred for a given application. We shall briefly discuss each type of these filters.

Butterworth Filters. The nth order Butterworth low-pass filter has the following characteristic function:

$$C(s) = \epsilon (s/\omega_\mathrm{p})^n$$

where ω_p is the passband edge frequency and ϵ is the passband ripple factor related to the maximum attenuation in the passband by $\alpha_\mathrm{pmax} = 10 \log(1 + \epsilon^2)$. The first $n - 1$ derivatives of the characteristic function are zero at the origin. For this reason, the attenuation response has the special characteristic that it is maximally flat at the frequency origin. The Butterworth filter has all of its attenuation zeros and poles at the frequencies zero or infinity. This leads to a less steep transition region from the passband to the stopband and results in a high filter order that is required to satisfy the attenuation requirements in both the passband and stopband. The polynomial characteristic function of the Butterworth filter leads to a transfer function having a constant numerator. This type of filters is called all-pole low-pass filters. For the Butterworth filter, Eq. (7) can be solved analytically. Thus, S_{21} and S_{11} can be written in analytical forms. In particular,

$$S_{11} = R_1 \frac{(\epsilon^{1/n} s/\omega_\mathrm{p})^n}{\displaystyle\sum_{i=0}^{n} a_i (\epsilon^{1/n} s/\omega_\mathrm{p})^i}$$

where the coefficients $a_0 = 1$ and a_i ($i = 1, 2, \ldots, n$) are given by

$$a_i = \prod_{\kappa=1}^{i} \frac{\cos\gamma_{k-1}}{\sin\gamma_k} \qquad \text{with} \quad \gamma_k = k\pi/2n$$

According to Eq. (9b), the input impedance function Z_in can be readily determined and then expanded into a continued fraction at infinity according to the first Cauer canonical form (8a). The resulting LC ladder filter is illustrated in Fig. 3, where the minimum inductor structure is selected. It is noted that the minimum capacitor structure is available as the dual network to the minimum inductor structure. The LC values of the resulting ladder filter can be determined either according to the continued fraction expansion of Eq. (8a) or by using explicit formulas, which are available for all-pole filters (15). Such formulas are especially simple for frequency and impedance normalized filters, for which the edge frequency of the passband, the source terminating resistor, and the load terminating resistor (where possible) are normalized to unity. The LC element formula for the nth-order minimum inductor Butterworth ladder filter is given by

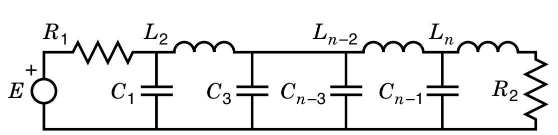

Figure 3. Minimum inductor ladder structure for all-pole filters. The number of inductors is equal to (when $L_n \neq 0$) or less than (when $L_n = 0$ and $C_{n-1} \neq 0$) the number of capacitors.

$$\left.\begin{array}{r} C_m\,(m\,\text{is odd}) \\ L_m\,(m\,\text{is even}) \end{array}\right\} = 2\epsilon^{1/n} \sin\gamma_{2m-1} \quad \text{and} \quad m = 1, 2, \ldots, n$$

Chebyshev Filters. The characteristic function of the Chebyshev filter is a Chebyshev polynomial, which can be written in a compact form as follows:

$$C(\omega/\omega_\mathrm{p}) = \epsilon T_n(\omega/\omega_\mathrm{p}) = \epsilon \begin{cases} \cos(n \cos^{-1} \omega/\omega_\mathrm{p}) & \text{for } |\omega/\omega_\mathrm{p}| \le 1 \\ \cosh(n \cosh^{-1} \omega/\omega_\mathrm{p}) & \text{for } |\omega/\omega_\mathrm{p}| \ge 1 \end{cases}$$

where $T_n(\omega)$ is the nth-order Chebyshev polynomial. Therefore, the Chebyshev filter is an all-pole low-pass filter, having all attenuation poles at infinity. In the passband, however, the Chebyshev filter has attenuation zeros at the finite frequencies and the attenuation function has an equiripple form. Because of the optimally distributed attenuation zeros in the passband, the Chebyshev filter has a steeper transition region than the Butterworth filter so that the Chebyshev filter can satisfy the same attenuation requirements with a much lower filter order than the Butterworth filter. For example, an eighth-order Chebyshev filter may satisfy the practical attenuation requirements that would require a 20th-order Butterworth filter. However, it is also noted that because of the maximum flat property, Butterworth filters have a much smoother phase/delay response than Chebyshev filters, leading to lower time-domain distortion of passband signals.

The LC ladder synthesis of Chebyshev filters can be achieved in the same way as for Butterworth filters and the synthesized two-ports also have the same ladder structures as illustrated in Fig. 3. The explicit formulas for LC ladder component values of an nth-order Chebyshev filter are given with help of two intermediate constants h and η (15) as follows:

$$h = \left[\frac{1}{\epsilon} + \left(1 + \frac{1}{\epsilon^2}\right)^{1/2}\right]^{1/n} \quad \text{and} \quad \eta = \left(h - \frac{1}{h}\right)$$

$$C_1 = \frac{4 \sin\gamma_1}{\eta R_1} \quad \text{with} \quad \gamma_m = m\pi/2n$$

$$C_{2m-1} L_{2m} = \frac{16 \sin\gamma_{4m-3} \sin\gamma_{4m-1}}{\eta^2 + 4\sin^2\gamma_{4m-2}}, \qquad m = 1, 2, \ldots, n/2$$

$$C_{2m+1} L_{2m} = \frac{16 \sin\gamma_{4m-1} \sin\gamma_{4m+1}}{\eta^2 + 4\sin^2\gamma_{4m}}, \qquad m = 1, 2, \ldots, n/2$$

$$C_n = \frac{4 \sin\gamma_1}{\eta R_2} \qquad \text{for odd}\, n$$

$$L_n = \frac{4 R_2 \sin\gamma_1}{\eta} \qquad \text{for even}\, n$$

Inverse Chebyshev Filters. The inverse Chebyshev filters have the reverse passband and stopband behavior with respect to the Chebyshev filters. The passband of the inverse Chebyshev filter is maximum flat at the origin and the stopband has the equiripple form. The characteristic function for inverse Chebyshev filters can be written as

$$C(s) = 1/\epsilon T_n(\omega_\mathrm{p}/\omega)$$

where T_n is the nth Chebyshev polynomial. For the LC ladder synthesis of the inverse Chebyshev filter, which has finite-frequency attenuation poles, the continued fraction expansion technique can be generalized by allowing the removal of simple resonant circuit branches that have resonant frequencies in one-to-one correspondence with the finite frequencies of attenuation poles. However, this poses a potential problem such that, during the generalized continued fraction expansion, the removal of a finite frequency pole requires shifting a zero of the remaining input impedance/admittance to the same frequency as the attenuation pole that is to be removed. This so-called zero-shifting process can introduce a negative LC element value that can be absorbed into a Brune section after the pole removal. Fortunately, there is a way around this problem of physically unrealizable negative LC elements if the filter has an attenuation pole at infinity, such as the odd-order inverse Chebyshev filter. In this case, the zero-shifting can be achieved by the so-called partial removal of the infinity attenuation pole. The resulting LC ladder two-port is no longer a canonical network and no longer contains Brune sections.

A fifth-order inverse Chebyshev filter can have an implementation such as that shown in Fig. 1(a), where the two left-hand shunt capacitors only partially remove the attenuation pole at infinity and the right-hand shunt capacitor finally removes this pole completely. For the even-order inverse Chebyshev filters, which do not have attenuation poles at infinity, a frequency transformation, which will be discussed in the next section, should be performed before the synthesis process in order to introduce an attenuation pole at infinity.

Because LC ladder implementations of inverse Chebyshev filters are not canonical networks, they require a larger number of LC elements than do Chebyshev filters of the same order. Furthermore, because the transition region of both types of filters are similar with regard to their transition-band steepness, the Chebyshev filter is usually preferred to its inverse version. However, the inverse Chebyshev filter has a better phase/delay response due to its maximally flat passband. Therefore, it may be preferred if a smooth delay response is required.

Elliptic Filters. The elliptic filter has equiripple attenuation in both the passband and stopband. It provides the lowest filter order satisfying a given attenuation requirement. For comparison, a sixth-order elliptic filter can satisfy the same attenuation requirement that would require an eighth-order Chebyshev filter. The characteristic function for the nth-order elliptic filter is a Chebyshev rational function given by

$$C(s) = \epsilon d \begin{cases} s\displaystyle\prod_{i=0}^{m} \frac{s^2+\omega_{0,2i}^2}{s^2+\omega_{\infty,2i}^2} & \text{for } n = 2m+1 \\ \displaystyle\prod_{i=0}^{m} \frac{s^2+\omega_{0,2i-1}^2}{s^2+\omega_{\infty,2i-1}^2} & \text{for } n = 2m \end{cases}$$

where d is a scaling constant such that the passband ripple factor is once again ϵ and the attenuation zeros $\omega_{0,j}$ and poles $\omega_{\infty,j}$ are calculated by means of the elliptic functions, which are discussed in many filter design books (19). The attenuation zeros and poles of an elliptic characteristic function are located symmetrically around a frequency ω_t in the transition band such that $\omega_{0,j}\omega_{\infty,j} = \omega_\mathrm{t}^2$. This frequency ω_t is a measure of the selectivity of the filter. The synthesis process for elliptic filters is very similar to that for inverse Chebyshev filters. In particular, the LC ladder network in Fig. 1(a) can be used to implement a fifth-order elliptic filter.

Thomson Filters. All of the above filter types are designed to meet specified attenuation requirements. The Thomson filter, on the other hand, achieves maximally flat group delay by maintaining the first n derivatives of the group delay to be zero at the frequency origin. The transfer function of Thomson filters is an all-pole function with the Bessel polynomial as the denominator:

$$S_{21}(s) = \frac{B_n(0)}{B_n(s)}$$

where

$$B_n(s) = \sum_{i=0}^{n} \frac{(2n-1)!s^i}{2^{n-i}i!(n-i)!}$$

The normalized group delay of the Thomson filter approximates unity in the neighborhood of the frequency origin. The higher the filter order n, the wider the frequency band over which a flat delay response is achieved. The time-domain responses of the Thomson filter are very smooth. For example, the step response has no overshoot. The synthesis of Thomson filters is similar to that for other all-pole filters.

It is noted that all the prototype filters discussed so far allow a closed-form solution for the filter approximation problem. The filter approximation of more general filter types such as filters with nonequiripple attenuation/phase behavior may be solved in a satisfactory manner by using computer-aided numerical methods.

Frequency Transformations

In the previous sections, we discussed various types of low-pass prototype filters. The approximation solutions and the filter structures of these prototype filters can also be used to obtain other filter types by means of appropriate frequency transformations.

Frequency Scaling. Low-pass prototype designs are usually obtained for normalized case so that the passband edge frequency is normalized to unity. This is especially the case when the explicit design formulas are used. To denormalize the passband edge to a specified value ω_p, the following frequency transformation can be used:

$$p = s/\omega_\mathrm{p}$$

where p is the complex frequency before transformation. The filter structure does not change after the denormalization, but the LC element values of a given filter structure are scaled accordingly.

Low-Pass to High-Pass Transformation. A high-pass filter can be obtained the following frequency transformation:

$$p = \omega_\mathrm{p}/s$$

which results in replacing each inductor with a capacitor and vice versa.

Low-Pass to Bandpass Transformation. The specification of a bandpass filter is given by the two passband edges ω_{pl} and ω_{ph} ($\omega_{\mathrm{pl}} < \omega_{\mathrm{ph}}$) and the two stopband edges ω_{sl} and ω_{sh} ($\omega_{\mathrm{sl}} < \omega_{\mathrm{sh}}$). The bandpass characteristic can be thought of as a combination of a low-pass and a high-pass characteristic such as

$$p = \frac{s}{(\omega_{\mathrm{ph}} - \omega_{\mathrm{pl}})} + \frac{\omega_{\mathrm{pl}}\omega_{\mathrm{ph}}/(\omega_{\mathrm{ph}} - \omega_{\mathrm{pl}})}{s} \tag{10}$$

The stopband edges ω_{sl} and ω_{sh} can be calculated using Eq. (10) by setting p equal to the low-pass prototype stopband edge. Because Eq. (10) is a second-order equation in s, it determines both stopband edges ω_{sl} and ω_{sh}. Therefore, these stopband edges are not independent of each other but related by $\omega_{\mathrm{pl}}\omega_{\mathrm{ph}} = \omega_{\mathrm{sl}}\omega_{\mathrm{sh}}$, resulting in a frequency-domain symmetrical bandpass filter. According to Eq. (10), a bandpass filter structure is obtained from its low-pass prototype by replacing each inductor with a series resonant circuit and each capacitor with a parallel resonant circuit.

A minor problem can arise from the direct application of Eq. (10) to a parallel or series resonant circuit, such as the parallel resonant circuit in Fig. 1(a), when transforming an inverse Chebyshev or an Elliptic low-pass filter into the corresponding band-pass filter. The transformed resonant circuit, which is a combination of a parallel and a series resonant circuits, does not directly relate to the anticipated attenuation poles, resulting in a less favorable stopband sensitivity. This problem can be resolved by using network transformations such that a parallel resonant circuit transforms into two parallel resonant circuits in series while a series resonant circuit transforms into two series resonant circuits in parallel.

Low-Pass to Band-stop Transformation. The band-stop filter can be obtained from a bandpass filter by interchanging its passband with its stopband frequency location. Therefore, the band-stop characteristic can be obtained by performing a bandpass transformation on a high-pass filter instead of a low-pass filter, resulting in the low-pass to band-stop transformation

$$p = \left(\frac{s}{(\omega_{\mathrm{ph}} - \omega_{\mathrm{pl}})} + \frac{\omega_{\mathrm{pl}}\omega_{\mathrm{ph}}/(\omega_{\mathrm{ph}} - \omega_{\mathrm{pl}})}{s}\right)^{-1}$$

Because of the similarity between the bandpass and band-stop transformations, the properties discussed above for the band-pass transformation can be easily rewritten for the band-stop transformation.

Other Frequency Transformations. The frequency transformations discussed so far are reactance transformations; that is, they transform a reactance into another reactance. Whereas reactance transformations are very useful, nonreactance transformations are often required to transform a characteristic function that is not realizable as an LC ladder two-port into a realizable one.

The even-order elliptic filter has the property that its attenuation has a nonzero value at the origin and a finite value at infinity. However, a practical LC ladder implementation requires an attenuation pole at infinity. Furthermore, it is often desirable to have the zero attenuation at the dc level, which also allows for a balanced load resistance equal to the source resistance. In order to achieve these requirements, the following transformation can be applied to the characteristic function before the synthesis process:

$$s^2 = \omega_\mathrm{p}^2 \frac{\omega_\infty^2 - \omega_\mathrm{p}^2}{\omega_\mathrm{p}^2 - \omega_0^2} \cdot \frac{p^2 + \omega_0^2}{p^2 + \omega_\infty^2}$$

where ω_0, ω_p, and ω_∞ are respective frequencies for the first passband attenuation zero, the passband edge, and the last finite-frequency attenuation pole. This transformation transforms the passband attenuation zero at ω_0 to the origin, the stopband attenuation pole at ω_∞ to infinity, while retaining the passband edge at ω_p. In general, the transformed filter has a poorer performance (especially in the transition region) than the original elliptic filter, because the latter is the optimum solution. However, the transformed filter still has a better performance than an original elliptic filter of lower order.

The even-order Chebyshev filters do not have an attenuation zero at the origin while having attenuation poles at infinity. The above transformation can be modified to just move the attenuation zero at ω_0 to the origin:

$$s^2 = \frac{\omega_\mathrm{p}^2}{\omega_\mathrm{p}^2 - \omega_0^2}(p^2 + \omega_0^2)$$

Similarly, for even-order inverse Chebyshev filters, the attenuation pole at ω_∞ can be moved to infinity by the following transformation:

$$s^2 = (\omega_\infty^2 - \omega_\mathrm{p}^2)\frac{p^2}{p^2 + \omega_\infty^2}$$

ACTIVE INTEGRATED CIRCUIT IMPLEMENTATIONS OF *LC* LADDER FILTERS

In the following sections, we discuss various techniques for the design of RC-active filters that are derived from LC ladder filters. However, the design details and parasitic effects (primarily due to the finite gain and bandwidth of the op-amps) are not discussed. Reference material on these topics can be found in the related articles in this encyclopedia and in Refs. 20–24.

RC-Active Ladder Filters Based on Simulating Inductors

The RC-active filters in this category can be readily obtained by replacing inductors with selected active circuits. Three basic types of active circuits are employed and discussed in the following.

Gyrators. A classical approach to the replacement of inductors with active circuits is to use a two-port gyrator termi-

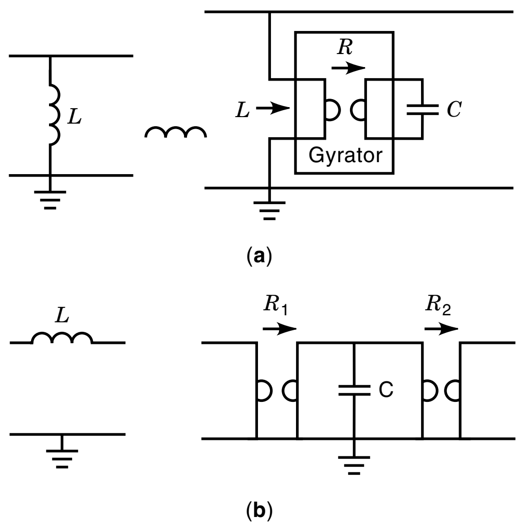

Figure 4. (a) Grounded-inductor simulation as may be used in high-pass filters. (b) Floating-inductor simulation as may be used in low-pass filters. Both inductor simulations use a gyrator, which is realized by an active circuit.

nated at one end with a capacitor C as shown in Fig. 4(a). In general, the relationship between the input impedance at port 1, Z_{in}, and the terminating impedance, Z_{ld}, at port 2 of a gyrator is given by

$$Z_{\mathrm{in}} = R^2/Z_{\mathrm{ld}}$$

where R is the gyration resistance inherent to the gyrator circuit. Therefore, the inductance seen from port 1 is given by $L = R^2C$.

There are two types of topological situations involving the use of inductors, namely grounded inductors and floating inductors, as shown in Figs. 4(a) and 4(b), respectively. To simulate a grounded inductor, a one-port grounded gyrator may be employed; and to simulate a floating inductor, a two-port grounded gyrator is needed. Note that because the active gyrator circuits involve complicated active circuitry, minimum inductor implementations should be chosen in order to minimize the number of required gyrators.

In general, passive implementations of gyrators are not available for many applications. In the RC-active filter application, small-signal active implementations of gyrators have been specifically designed for converting a capacitor to an inductor (25–27). When the gyrator is used as an impedance converter, it may be considered as a special case of the generalized impedance converter (GIC), which is discussed in the following.

Generalized Impedance Converters. The GIC is a two-port circuit, usually employing two op-amps as shown in Fig. 5(a), where the impedances Z_i are usually either a resistor or a capacitor. The impedance relations between the input and terminating impedances of a GIC are given by

$$Z_{\mathrm{in1}} = \frac{Z_1Z_3}{Z_2Z_4} Z_{\mathrm{ld2}} \tag{11a}$$

or

$$Z_{\mathrm{in2}} = \frac{Z_2Z_4}{Z_1Z_3} Z_{\mathrm{ld1}} \tag{11b}$$

Therefore, choosing

$$Z_1 = R_1, \quad Z_2 = R_2, \quad Z_3 = R_3, \quad Z_4 = 1/sC_4, \quad \text{and} \quad Z_{\mathrm{ld1}} = R_5 \tag{12}$$

leads to a simulated grounded inductance at port 1 with $L = R_1R_3C_4R_5/R_2$.

According to Eq. (11a), Z_2 could be chosen as a capacitor instead of Z_4. However, for practical reasons the choice in Eq. (12) has a better performance at high frequencies.

In general, we can define a conversion factor $K(s) = Z_1(s)Z_3(s)/Z_2(s)Z_4(s)$, where $Z_i(s)$ can be any impedance functions. Thus, the GIC can perform more general impedance conversion than the inductance simulation. In particular, if port 1 is terminated in a capacitor C_{ld1}, the input impedance at port 2 is given by

$$Z_{\mathrm{in2}} = \frac{R_2}{R_1R_3C_4C_{\mathrm{ld1}}s^2}$$

which is a so-called frequency-dependent negative resistance (FDNR). Applications of FDNRs are discussed in the next subsection.

The GIC is used in a very similar way to that of a gyrator. In particular, the gyrator simulating a grounded inductor, as shown in Fig. 4(a), can be replaced with a GIC given by Eq. (12). The GICs can also be used to simulate floating inductors as shown in Fig. 5(b), which was first proposed by Gorski-Popiel. It is noted that, unlike the gyrator, the GICs with the

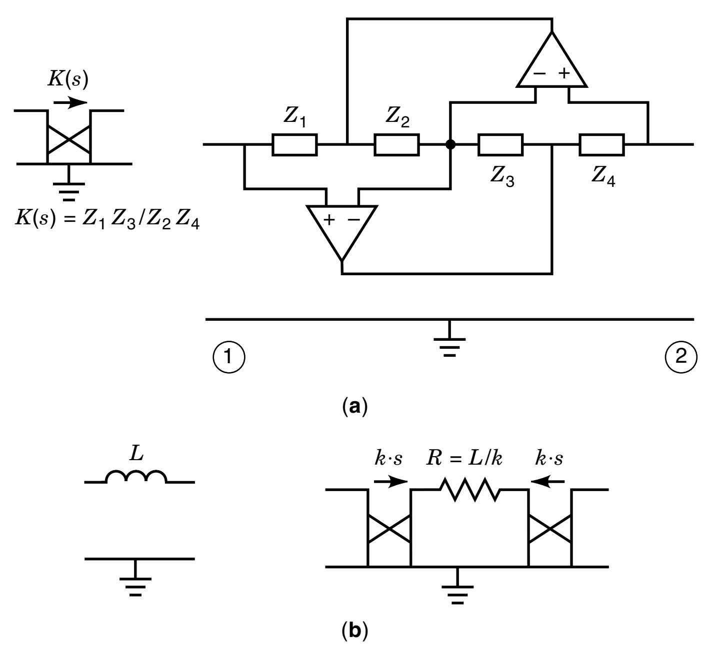

Figure 5. (a) Active implementation of GIC and its corresponding symbol. $K(s)$ is the conversion factor. (b) Floating-inductor simulation using GIC. This simulation uses a resistor connecting two GICs. The required capacitors are hidden in the GICs.

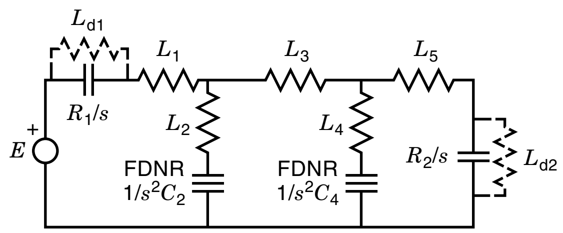

Figure 6. A fifth-order RC-active filter using FDNRs. The dashed resistors L_{d1} and L_{d2} are the add-on discharging resistors.

conversion factor $k \cdot s$ (k is a constant) convert a floating inductor into a floating resistor whereas the required capacitors are embedded in the GICs.

Frequency-Dependent Negative Resistors. All of the above RC-active filters use minimum inductor implementations. The minimum capacitor implementations can also be employed in an effective way if the concept of the FDNR is used. The dimensionless filter transfer function of any LCR network is unaltered if each branch is scaled by a uniform function. Thus, impedance scaling all branches by $1/s$ converts all inductors to resistors, all resistors to capacitors, and all capacitors to FDNR elements. An example of a RC-active filter using FDNRs is given in Fig. 6, where the dual network to the fifth-order filter in Fig. 1(a) is $1/s$ impedance-scaled. The resulting FDNRs can be implemented using GICs. It is noted that the filter network in Fig. 6 is no longer resistively terminated, which may cause a practical dc bias problem if the source and/or load are not resistively coupled to ground. This termination problem can be resolved by inserting two unity-gain amplifiers between the source and the load, and the bias current problem can be compensated for by connecting two discharging resistors across the capacitors, as shown in Fig. 6. The values of these resistors are suggested to be chosen such that the filter attenuation at the dc level remains equal to unity, that is,

$$L_{d2} = L_{d1} + L_1 + L_2$$

and that the insertion of L_{d1} and L_{d2} introduces the least distortion of the filter frequency response.

RC-Active Filters Based on Simulating Ladder SFGs

The design and implementation of RC-active filters based on simulating the voltage–current signal flow graphs (SFGs) of LC ladder prototype structures was proposed by Girling and Good. An SFG can be derived for any given LC ladder filter, where for the purpose of implementing RC-active filters, the SFG should be arranged in such a way that it consists only of inverting/noninverting integrators, analog multipliers, and adders. An inductor is represented in the SFG according to

$$I_{\text{out}} = \frac{1}{sL} V_{\text{in}}$$

and a capacitor according to

$$V_{\text{out}} = \frac{1}{sC} I_{\text{in}}$$

so that all the reactive components are represented as integrators within the SFG. The terminating resistors are represented by constant-valued analog multipliers within the SFG. The physical interconnections of the LCR elements constrain the voltage and current signals to obey Kirchhoff's laws and are represented in the SFG by appropriate combinations of analog inverters and adders. An example of an SFG for the third-order low-pass filter in Fig. 3 (where $n = 3$) is given in Fig. 7(a), which is often referred to as the leapfrog structure. It is noted that all inductors are simulated by noninverting integrators, and all capacitors are by inverting integrators so that all signals entering an adder have the same positive sign. Furthermore, because all summations are performed immediately prior to integration, summation can be easily achieved in the RC-active circuit by current-summing at the virtual ground input terminals of the integrator's op-amps. Thus, no dedicated summing devices are required. In Fig. 7(b), the complete circuit corresponding to the SFG in Fig. 7(a) is given for the selected type of integrator implementations, where the circuit parameters can be determined by

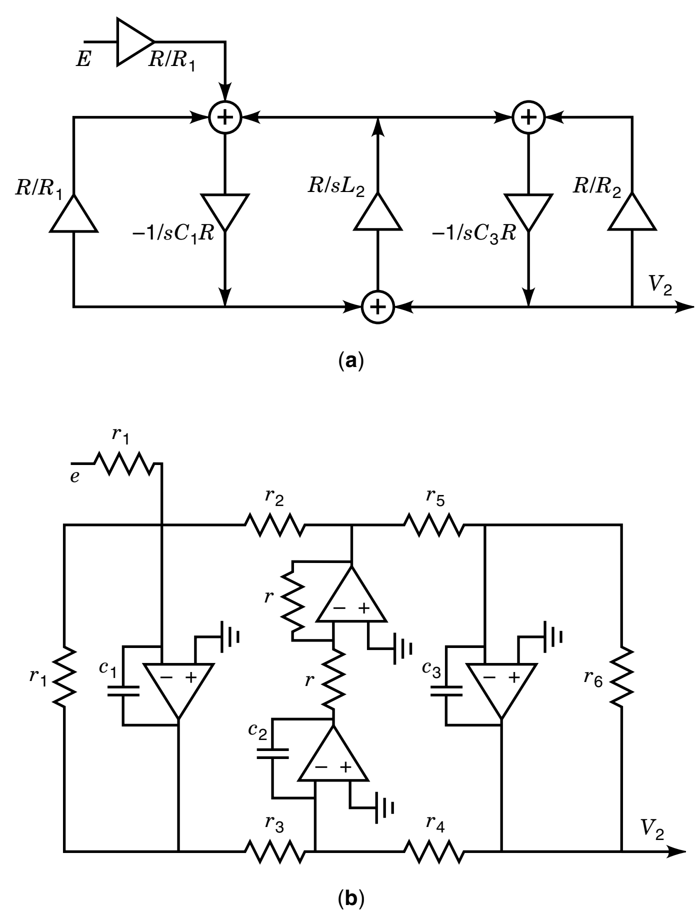

Figure 7. (a) A third-order leapfrog SFG scaled by a constant R. (b) The corresponding complete RC-active circuit, where $c_1r_1 = C_1R_1$, $c_1r_2c_2r_3 = C_1L_2$, $c_2r_5c_3r_4 = L_2C_3$, $c_3r_6 = C_3R_2$. No dedicated summing devices are needed.

comparing the loop gains between the circuit representations in Figs. 7(a) and 7(b). Note that other types of integrator implementations may be chosen, depending on the frequency range within which the circuit is intended to operate.

The SFG simulation method is very straightforward and easy to use, especially when designing band-pass filters. However, it is noted that, when drawing the SFGs for *LC* ladder network that contain a π circuit of capacitors or a T circuit of inductors, difficulties arise because two adjacent SFG blocks have ports with the same orientation facing or leaving each other. This problem can be solved perfectly by using network transformations involving Brune sections in the same way as it has been done for LDI/LDD digital filters (28). By now, it is evident that the Brune section is a very useful building block in *RC*-active and digital filter implementations, although it is, strictly speaking, not a ladder component.

DISCRETE-TIME SC AND DIGITAL IMPLEMENTATIONS OF *LC* LADDER FILTERS

Both the SC filter and digital filter are sampled data (discrete-time) systems. The frequency response of a discrete-time system is adequately described in the z domain with $z = e^{sT}$, where s is the complex frequency and T is the sampling period. The frequency-domain design methods for SC filters and for digital filters have many similarities and often have the same z-domain transfer functions, in spite of the fact that SC filters are implemented as analog circuits whereas digital filters employ the digital arithmetic operations of addition, multiplication, and delay and are implemented as computer programs or by dedicated hardware.

The frequency-domain design of discrete-time SC and digital filters can be performed directly in the z domain. However, high-performance discrete-time filters may be designed by simulating continuous-time *LC* ladder filters as discrete-time filters. This is achieved in a way such that all of the abovementioned favorable stability and sensitivity properties of *LC* filters are preserved. The transfer functions of the continuous-time *LC* ladder filter and its discrete-time counterparts are related by the bilinear transformation

$$s = (z - 1)/(z + 1)$$

In the following, we briefly discuss methods for converting continuous-time *LC* ladder filters into their discrete-time counterparts. The design details for SC and digital filter circuit components and the treatment of parasitic and other nonideal effects are not considered here. Reference material on these topics can be found in the related articles in this encyclopedia and in Refs. 11 and 28–32.

Switched Capacitor Filters

SC filters that are based on *LC* ladder filters can be derived from *RC*-active filters that are themselves derived from *LC* ladder filters, preferably using the SFG simulation technique. In fact, the resistors in *RC*-active ladder filters can be simulated by switched capacitors, leading directly to the SC filter. There is a variety of different SC circuits for simulating the resistors in *RC*-active ladder filters. Different SC resistor circuits, which are used to replace resistors in *RC*-active filters, may result in different frequency-domain relationships between the transfer functions of the continuous-time *LC* ladder filter and its discrete-time SC counterpart. An example of SC resistor circuits is given in Fig. 8(a), which leads to the desired frequency-domain relationship given by the bilinear transformation.

In many SC filters, the ideal circuit capacitances are not significantly larger than the parasitic capacitances. In fact, the latter is around 20% of the former. Therefore, it is extremely critical to only use those SC circuits that are not sensitive to parasitic capacitances. An example of a so-called stray-insensitive SC resistor circuits is given in Fig. 8(b). This circuit yields a different frequency transformation than the bilinear transformation. In order to achieve the desired bilinear transformation using simple SC ladder circuits, a so-called predistortion technique may be used that adds a positive capacitance to one circuit component and subtracts an equal-valued negative capacitance from another circuit component, along with an impedance-scaling technique (30). It is noted that a similar technique is also used for LDI/LDD digital filters.

Another alternative approach for designing SC filters is to directly simulate each inductor and each terminating resistor in the *LC* ladder filter. In this method, the interconnections of capacitors and simulated inductors/resistors are achieved by the so-called voltage inverter switchs (VIS), which contain active op-amps. This component simulation method guarantees the bilinear transformation between transfer functions of the continuous-time *LC* ladder filter and its discrete-time SC counterpart, which can be designed insensitive to parasitic capacitances. Nevertheless, considerable design effort and/or complicated switching signals may be required to achieve the low-sensitivity property.

Digital Ladder Filters

In a way that is similar to the SC simulation of *LC* ladder filters, there are two alternative approaches for the digital simulation of *LC* ladder filters, namely the simulation of each *LCR* component and the simulation of the SFG representation.

The component simulation method is achieved using wave digital filters (WDF) (11), where the circuit components of the *LC* ladder filter, such as inductors, capacitors and resistors, are directly simulated by corresponding digital domain components, such as delay registers and inverters. The parallel and serial interconnections of these digital components are facilitated by so-called parallel and serial adapters that contain adders and multipliers. A distinguishable advantage of

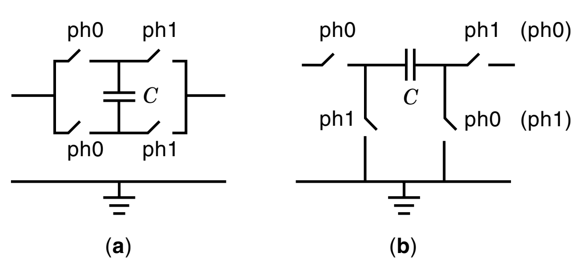

Figure 8. (a) Bilinear SC resistor circuit with two switching phases. (b) Stray-insensitive SC resistor circuit which can be used to form inverting or noninverting (switching scheme in parentheses) integrators.

WDFs is that internal passivity is maintained under both infinite and finite wordlength conditions. This leads to the suppression of parasitic oscillations that are caused by overflow and underflow operations.

The SFG simulation of *LC* ladder filters employs lossless digital integrators and/or lossless digital differentiators (LDIs/LDDs) to replace the corresponding integration/differentiation operations in the continuous-time ladder SFG (28,31,32), where the continuous-time SFG may first be predistorted and impedance scaled in such a way that delay-free loops are avoided and all inductors and capacitors are individually and directly realized as discrete-time LDI/LDD elements. Each LDI/LDD element contains a delay register, a multiplier, and an adder. This SFG simulation approach does not require any special interconnection components and retains the one-to-one correspondence between the *LC* ladder filter parameters and its LDI/LDD digital counterparts. A distinguishing advantage of LDI/LDD ladder filters is that all of the state variables of inductor-simulating or capacitor-simulating LDI/LDD elements are independent of each other, thereby allowing concurrent implementation in parallel arithmetic schemes and flexible scheduling in bit-serial arithmetic schemes. It is noted that the very useful Brune sections can be perfectly implemented using the LDI/LDD method.

BIBLIOGRAPHY

1. V. Belevitch, Summary of the history of circuit theory, *Proc. IRE,* **50** (5): 848–855, 1962.
2. S. Darlington, A history of network synthesis and filter theory for circuits composed of resistors, inductors, and capacitors, *IEEE Trans. Circuits Syst.,* **CAS-31**: 3–13, 1984.
3. A. Fettweis, Filters met willekeurig gekozen dempingspolen en Tschebyschewkarakteristiek in het doorlaatgebied, *Tijdschrift van het Nederlands Radiogenootschap,* **25**, sec. 8, no. 5–6, pp. 337–382, 1960.
4. H. J. Orchard, Inductorless filters, *Electron. Lett.,* **2**, 224–225, 1966.
5. E. Christian, *LC Filters: Design, Testing, and Manufacturing,* New York: Wiley, 1983.
6. R. H. S. Riordan, Simulated inductors using differential amplifiers, *Electron. Lett.,* **3** (2): 50–51, 1967.
7. M. S. Ghausi, Analog active filters, *IEEE Trans. Circuits Syst.,* **CAS-31**: 13–31, 1984.
8. A. Fettweis, Switched-capacitor filters: From early ideas to present possibilities, *Proc. IEEE Int. Symp. Circuits Syst.,* Chicago, 414–417, April 1981.
9. G. C. Temes, MOS switched-capacitor filters—History and the state of the art, *Proc. Eur. Conf. Circuits Theory Design,* Den Haag, pp. 176–185, Aug. 1981.
10. W. K. Jenkins, Observations on the evolution of switched capacitor circuits, *IEEE Circuits Syst. Magazine,* Centennial Issue, 22–33, 1983.
11. A. Fettweis, Wave digital filters: Theory and practice, *Proc. IEEE,* **74**: 270–327, 1986.
12. A. Fettweis, Digital circuits and systems, *IEEE Trans. Circuits Syst.,* **CAS-31**, pp. 31–48, 1984.
13. R. Saal and W. Entenmann, *Handbook of Filter Design,* Berlin: AEG Telefunken, 1979.
14. A. Zverev, *Handbook of Filter Synthesis,* New York: Wiley, 1967.
15. A. S. Sedra and P. O. Brackett, *Filter Theory and Design: Active and Passive,* Champaign, IL: Matrix Publishers Inc., 1978.
16. W. K. Chen, *Passive and Active Filters: Theory and Implementations,* New York: Wiley, 1986.
17. G. C. Temes and J. W. LaPatra, *Circuit Synthesis and Design,* New York: McGraw-Hill, 1977.
18. V. Belevitch, *Classical Network Theory,* San Francisco: Holden-Day, 1968.
19. R. W. Daniels, *Approximation Methods for Electronic Filter Design,* New York: McGraw-Hill, 1974.
20. G. C. Temes and S. K. Mitra (eds.), *Modern Filter Theory and Design,* New York: Wiley, 1973.
21. G. S. Moschytz, Inductorless filters: A survey. I. Electromechanical filters. II. Linear active and digital filters, *IEEE Spectrum,* **7** (8): 30–36, 1970; **7** (9): 63–75, 1970.
22. S. K. Mitra (ed.), *Active Inductorless Filters,* New York: IEEE Press, 1971.
23. L. P. Huelsman (ed.), *RC-Active Filters: Theory and Application,* Stroudsburg: Dowden, Hutchinson and Ross, 1976.
24. W. E. Heinlein and W. H. Holmes, *Active Filters for Integrated Circuits,* London: Prentice-Hall, 1974.
25. B. A. Shenoi, Practical realization of a gyrator circuit and *RC*-gyrator filters, *IEEE Trans. Circuit Theory,* **CT-12**: 374–380, 1965.
26. W. H. Holmes, S. Gruetzmann, and W. E. Heinlein, Direct-coupled gyrators with floating ports, *Electron. Lett.,* **3** (2): 46–47, 1967.
27. D. G. Lampard and G. A. Rigby, Application of a positive immitance inverter in the design of integrated selective filters, *Proc. IEEE,* **55**: 1101–1102, 1967.
28. X. Liu and L. T. Bruton, Improved LDI digital filters derived from analog *LC* ladder filters, *Signal Processing,* **46**: 147–158, 1995.
29. G. S. Moschytz, *MOS Switched-Capacitor Filters: Analysis and Design,* New York: IEEE Press, 1984.
30. M. S. Lee, G. C. Temes, C. Chang, and M. G. Ghaderi, Bilinear switched-capacitor ladder filters, *IEEE Trans. Circuits Syst.,* **CAS-28**: 811–822, 1981.
31. L. T. Bruton, Low-sensitivity digital ladder filters, *IEEE Trans. Circuits Syst.,* **CAS-22**: 168–176, 1975.
32. D. A. Vaughan-Pope and L. T. Bruton, Transfer function synthesis using generalized doubly terminated two-pair network, *IEEE Trans. Circuit Syst.,* **CAS-24**: 79–88, 1977.

XIAOJIAN LIU
Gennum Corp.
LEONARD T. BRUTON
University of Calgary

LADDER NETWORKS. See LATTICE FILTERS.
LADDER STRUCTURES. See LADDER FILTERS.
LAMPS, FILAMENT. See PHOTOMETRIC LIGHT SOURCES.
LAMPS, INCANDESCENT AND HALOGEN. See FILAMENT LAMPS.
LANGUAGE, CONTEXT-SENSITIVE. See CONTEXT-SENSITIVE LANGUAGES.
LANGUAGE IDENTIFICATION. See AUTOMATIC LANGUAGE IDENTIFICATION.
LANGUAGE ISSUES IN INTERNATIONAL COMMUNICATION. See INTERNATIONAL COMMUNICATION.
LANGUAGES. See CONTEXT-SENSITIVE LANGUAGES.
LANGUAGES, AI. See AI LANGUAGES AND PROCESSING.

LANGUAGES, FUNCTIONAL PROGRAMMING. See FUNCTIONAL PROGRAMMING.

LANS. See ETHERNET; LOCAL AREA NETWORKS.

LAPLACE TRANSFORM. See FOURIER TRANSFORM.